



OPEN

Evaluation of *Theobroma cacao* L. as a bioindicator for cadmium contamination through H_2O_2 electrochemical analysis

Lenys Fernández¹✉, Patricio Javier Espinoza-Montero¹✉, María José Gallegos-Lovato¹, Paulo Bustamante¹, Diego Bolaños-Méndez¹, Juan Diego Sampedro¹, Augusto Rodríguez², Andrea Ortega-Gallegos³ & Mónica Jadan³

The use of sedentary bioindicators, such as trees, in environmental contamination monitoring is receiving increased focus. This study evaluates *Theobroma cacao* L. as a bioindicator for cadmium (Cd) contamination by quantifying hydrogen peroxide (H_2O_2) as an oxidative stress marker in cellular suspensions exposed to $CdSO_4$. Chronoamperometric measurements using platinum electrodes indicated Cd accumulation in *T. cacao* L. and revealed a corresponding increase in H_2O_2 production up to a threshold level, beyond which cell apoptosis occurred. These findings support the potential of *T. cacao* L. as a bioindicator of Cd pollution. Moreover, H_2O_2 quantification via chronoamperometry demonstrated a rapid and effective method for detecting Cd-induced oxidative stress in plant systems. Future research should explore field applications, evaluate alternative plant species, and assess long-term responses under real environmental conditions to optimize this approach for large-scale biomonitoring.

Keywords Sedentary bioindicators, *Theobroma cacao*, Cadmium contamination, Oxidative stress, Chronoamperometry

Environmental biomonitoring is a crucial tool for assessing contamination risks and their impact on ecosystems. Among the various biomonitoring strategies, sedentary bioindicators—organisms that accumulate and reflect environmental contaminants—are especially useful for evaluating pollution levels over time¹. Plants in particular are widely used to monitor toxic metal contamination due to their ability to absorb and store hazardous elements from soil and water^{2,3}.

Ecuador has a strong agricultural and economic interest in cultivating cacao, or *Theobroma cacao* L. The country's fine aroma cacao is particularly highly valued in European markets for its distinct flavor and quality^{4,5}. While bioindicators are often associated with organisms like lichens and mollusks, which passively reflect environmental contamination, certain plant species can actively serve as effective localized biomonitoring of soil pollution. *T. cacao* L., known for its ability to bioaccumulate cadmium (Cd), offers valuable insights into toxic metal contamination in agricultural ecosystems. This is especially relevant in Ecuador, where Cd pollution stems from both natural and anthropogenic sources, including industrial discharges, vehicular emissions, and artisanal mining¹¹. Unlike traditional bioindicators, which are widely distributed across different environments, *T. cacao* L. is cultivated in specific agricultural regions, making it a particularly relevant indicator of pollution in economically important crops. Monitoring oxidative stress responses in cacao plants can provide an early warning of Cd exposure, facilitating the evaluation of soil contamination levels and potential risks to food safety. This localized approach to biomonitoring is crucial in regions where toxic metal accumulation threatens both agricultural productivity and compliance with international trade regulations.

Cadmium exposure severely affects plant morphology, causing stunted growth, chlorosis, and impaired photosynthesis, as well as damaging cellular structures such as membranes and DNA⁶⁻⁸. One of the primary physiological responses to Cd stress is oxidative stress, which triggers excessive production of reactive oxygen species (ROS), including superoxide anions (O_2^-), hydroxyl radicals ($\cdot OH$), and hydrogen peroxide (H_2O_2)⁹.

¹Escuela de Ciencias Químicas, Pontificia Universidad Católica del Ecuador, Quito, Ecuador. ²Instituto de Investigaciones Fisicoquímicas Teóricas y Aplicadas (INIFTA), La Plata, Argentina. ³Universidad de las Fuerzas Armadas ESPE, Sangolquí, Ecuador. ✉email: lmfernandez@puce.edu.ec; pespinoza646@puce.edu.ec

Notably, Cd exposure has been shown to significantly increase H₂O₂ levels in plant systems, making it a useful marker for oxidative stress.

Electrochemical techniques offer sensitive and rapid methods to detect ROS, providing advantages over traditional spectrophotometric and chromatographic approaches^{3,4}. In particular, chronoamperometry allows real-time monitoring of H₂O₂ production in plant cell suspensions, making it a reliable indicator of Cd-induced oxidative stress¹⁰.

Considering these factors, this study aimed to explore the potential of *T. cacao* L. as a sedentary bioindicator by quantifying H₂O₂ in cellular suspensions derived from seed explants exposed to Cd²⁺ ions. The suspensions were cultivated under controlled in vitro conditions utilizing a medium simulating the optimal environment for plant tissue development¹¹. While previous studies have investigated Cd accumulation in cacao-growing soils^{16,17}, research on the use of cacao as an active bioindicator remains limited^{12,13}. This study seeks to bridge that gap by exploring H₂O₂ quantification as a novel approach for assessing toxic metal contamination. The findings will contribute to understanding the role of cacao as an environmental sentinel and demonstrate the applicability of electrochemical techniques in the biomonitoring of toxic metal pollution. Such a methodology could provide a practical alternative for environmental monitoring, particularly in regions where conventional assessment methods are impractical or imprecise.

Materials and methods

Reagents

The following reagents were used in this study: calcium nitrate (PhytoTechnology Laboratories, analytical grade); potassium sulfate (Merk, analytical grade); Bacto agar (Biomark); Murashige & Skoog basal medium with vitamins (MS); 2,4-dichlorophenoxyacetic acid (2,4-D); 6-benzylaminopurine (6-BAP); dipotassium phosphate (99%, Merck, analytical grade); monopotassium phosphate (99.05%, Merck, analytical grade); H₂O₂ (30% v/v, Sigma-Aldrich), and sulfuric acid (Fischer, analytical grade). An electrode polishing kit (CH Instruments, Inc.) was also employed.

Equipment

Experiments were conducted using a laminar flow cabinet (Esco); autoclave (Tuttnauer); Olympus BX-41 microscope (Olympus Corporation); orbital shaker (WiseSheak); ultrasonic bath (Branson 3800); and a Neubauer chamber (AR Biotech). Electrochemical measurements were performed with a potentiostat (Biologic SP-150); ECLab software V11.26; platinum (Pt) working electrode; Ag/AgCl reference electrode (3 mol L⁻¹ KCl); and graphite rod counter electrode.

Preparation of *T. cacao* L. cell suspensions

T. cacao L. pods were collected in the town of Mindo, Ecuador, (latitude: -0.0506,

longitude: -78.7788) in the province of Pichincha. The fruit was transported to the laboratory in a portable refrigerator. The disinfection process involved extracting and rinsing the *T. cacao* L. seeds with distilled water to remove the mucilage completely, followed by washing with a chlorine solution, testing concentrations between 3.5 and 5% for 10 min. The seeds were then rinsed three times with distilled water inside a laminar flow chamber¹⁴.

Callus formation was induced using MS medium containing hydrated calcium nitrate (1967 mg L⁻¹), potassium sulfate (1559 mg L⁻¹), sucrose (40 g L⁻¹), 6-BAP (4 mg L⁻¹), 2,4-D (2 mg L⁻¹), and 7 g of agar¹⁵.

Subsequently, four explants per flask were planted in MS medium and stored at room temperature under dark conditions for 30 days to allow for callus multiplication¹⁴. The same culture medium was used for both multiplication of callus and sowing.

To prepare the cellular suspensions, approximately 1 g of the formed callus was added to 50 mL of the aforementioned MS growing medium (excluding the agar). The mixture then underwent orbital agitation¹⁵.

Cells were counted by taking a sample of the suspension inside the flow chamber, which was subsequently introduced into the Neubauer chamber. The cells were observed and counted using an Olympus BX-41 microscope. Cellular concentration (CC) was calculated using Eq. (1):

$$CC = \frac{\# \text{ viable cells}}{\# \text{ squares}} * \frac{64 \text{ squares}}{1 \text{ square}} * \frac{1 \text{ square}}{(length * height * depth) \text{ mm}^3} * \frac{1000 \text{ mm}^3}{1 \text{ cm}^3} \quad (1)$$

Hydrogen peroxide production assessment

The electrochemical system consisted of a Pt working electrode, a graphite rod counter electrode, and a Ag/AgCl (3 mol L⁻¹ KCl) reference electrode. The Pt working electrode was cleaned using successive mechanical polishing with alumina powder of decreasing grain sizes (1, 0.3, and 0.05 μm)¹⁶ for 3 min for each grain size. Subsequently, electrochemical cleaning was performed via cyclic voltammetry in a 0.5 mol L⁻¹ H₂SO₄ solution, with potentials ranging from -0.300 to 1.800 V vs. Ag/AgCl at a scan rate of 100 mV s⁻¹.

Chronoamperometric measurements were performed in cell suspensions with a turbidity of 15 NTU and CC of 3 × 10⁴ cells mL⁻¹. Turbidity of initial cell solution 25 NTU and the CC of the stock solution was of 5 × 10⁴ cells mL⁻¹.

Calibration curves were constructed by measuring chronoamperometric currents in H₂O₂ standard solutions at concentrations ranging from 0.3 to 1.4 μmol L⁻¹ in a phosphate buffer solution (PBS) at pH 5.7. The standard addition method was employed to determine H₂O₂ concentrations to minimize the dependency between the target signal current and possible sample matrix interference²⁶. Method performance parameters, including sensitivity, detection limit, quantification limit, precision, and accuracy, were evaluated. The arithmetic mean,

standard deviation, coefficient of variation, and percent recovery (R%) were also calculated for the measurements ($n=5$). The percent coefficient of variation (CV%) values were assessed according to the acceptable limits described in the AOAC (2012) guidelines for laboratory chemical method validation in dietary supplements and botanicals. These were set at $CV < 11\%$ for reproducibility and precision and between 80 and 115% for R% values.

For the respective cellular stress experiments, 1:10 dilutions of aqueous suspensions were prepared using $CdSO_4$ concentrations of 5, 20, 50, and 100 $\mu\text{mol L}^{-1}$ ⁴. Cells were exposed to the stressing agent for 1, 2, 3, 4, 5, and 6 h. H_2O_2 quantification was performed using the standard addition method in a 0.1 mol L^{-1} PBS at pH 5.7. Aliquots of 20 μL were added from a 0.02 mol L^{-1} H_2O_2 standard solution every 20 s^{16,17}.

Results and discussion

Disinfection protocol for *T. cacao* L. explants

The most efficient disinfection protocol for *T. cacao* L. explants was determined by evaluating bacterial contamination, fungal contamination, and oxidation. The optimal method involved immersing the cacao seeds, with mucilage removed, in a 3.5% chlorine solution for 10 min (Table 1), followed by three rinses with distilled water in a laminar flow chamber. This approach minimized oxidation while effectively reducing microbial contamination, preventing inhibition of seed germination. This protocol aligns with reported plant tissue disinfection methods, where appropriate NaClO concentrations have been shown to reduce contamination without significantly affecting germination or development¹⁸. The selection of a 3.5% chlorine concentration effectively balanced microbial decontamination while maintaining explant viability, ensuring a suitable starting point for subsequent experimental procedures.

Induction and multiplication of embryogenic callus

Embryogenic callus formation in *T. cacao* L. seeds began seven days after sowing in MS medium. The calluses were kept in a dark environment to promote optimal growth. After 15 days, their successful development confirmed that the MS medium provided suitable conditions for explant cultivation (Fig. 1). After 30 days, an additional multiplication step was carried out using the same MS medium. Figure 1d shows the embryogenic callus alongside clusters of undifferentiated cells. The MS medium, enriched with macro- and micronutrients, vitamins, and cytokinins, created optimal circumstances for callus growth under in vitro conditions.

The induction and multiplication of embryogenic callus in *T. cacao* L. are critical steps in somatic embryogenesis and plant regeneration protocols. In this study, embryogenic callus formation began seven days after sowing in MS medium under dark conditions, consistent with established methodologies. Subsequent sub-culturing after one month further promoted callus proliferation.

The enriched MS medium provides essential support for in vitro plant tissue culture. The inclusion of plant growth regulators, such as 2,4-D, a synthetic auxin, and 6-BAP, a cytokinin, plays a key role in callus induction and somatic embryogenesis. Research has demonstrated that 2,4-D promotes cell division and dedifferentiation, while 6-BAP enhances cell proliferation and differentiation. Their synergistic effect has been shown to facilitate embryogenic callus development in cacao¹⁹.

Regular sub-culturing onto fresh medium is essential for maintaining cell viability, preventing necrosis, and ensuring continued callus proliferation. This practice replenishes nutrients and growth regulators while eliminating inhibitory metabolites. Studies have confirmed that sub-culturing enhances callus growth and embryogenic potential in cacao tissue cultures¹⁹.

Our results are consistent with those of previous studies highlighting the positive influence of 2,4-D and 6-BAP supplementation on callus development²⁰. To prevent cell death and aggregation, subcultures were periodically transferred to fresh medium²². Auxins such as 2,4-D are frequently used to induce embryogenic callus, as they regulate key physiological and molecular processes involved in somatic embryogenesis. Consistent with our observations, Hazuba-Przybył et al.²⁷ reported that the combination of 2,4-D and 6-BAP enhances somatic embryo formation from embryogenic callus structures.

Cell counting

Cell counting was conducted by taking a small aliquot from each suspension, placing it in the Neubauer chamber, and examining it under a microscope. Figure 2 shows optical microscope images of the cells at 10x magnification, showing fully disaggregated cells, confirming the suspensions were suitable for monitoring cell growth. Additionally, no large clusters of cells were observed.

	Chlorine concentration (%)	
Evaluated variables	3.5	5.0
Fungal contamination	10	12
Bacterial contamination	3.0	5
Oxidation	5.0	17

Table 1. Results of analyzed variables for determining optimal disinfection protocol.

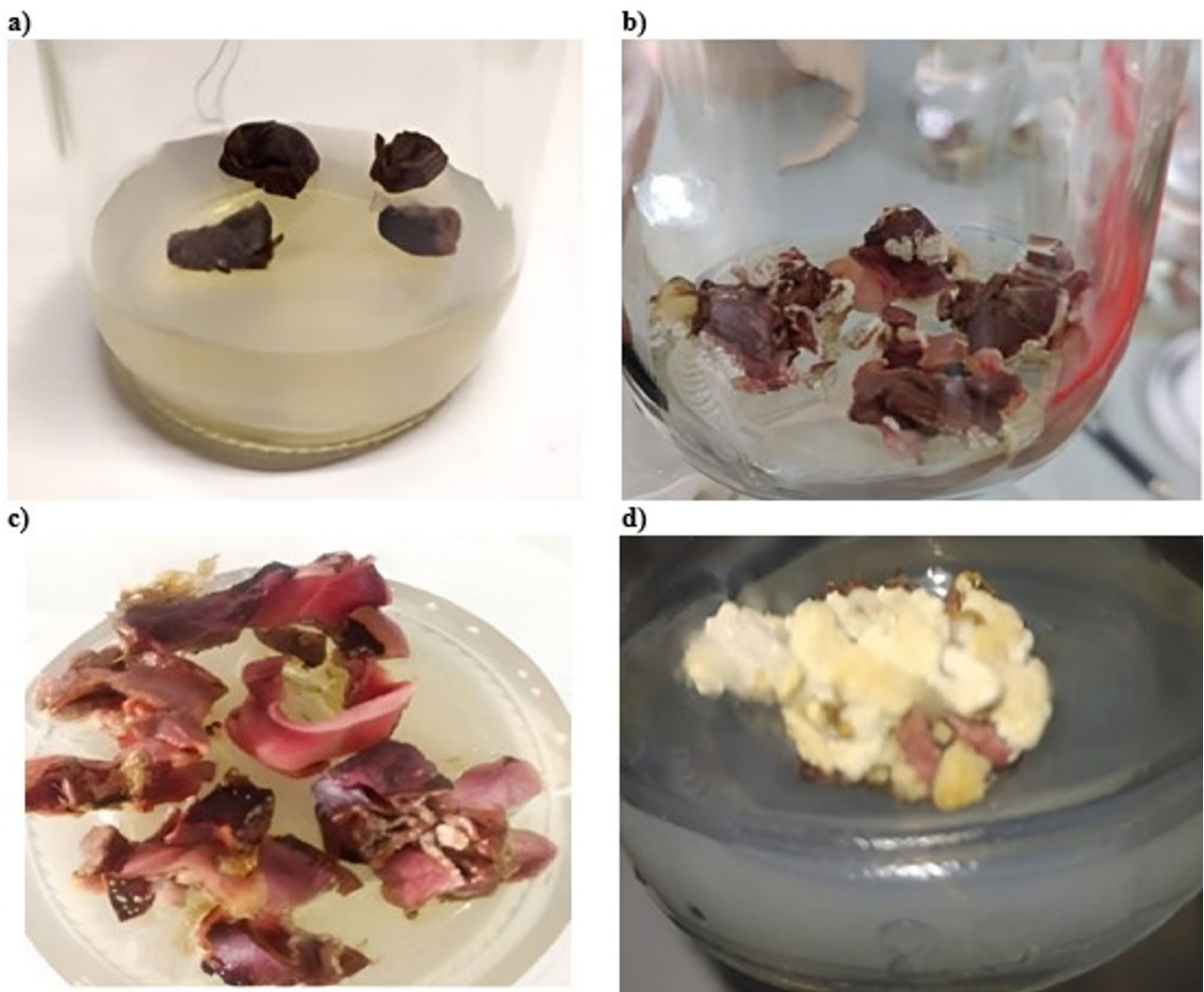


Fig. 1. *Theobroma cacao* L. seeds (a) immediately after sowing in the medium; (b), (c) callus formation 15 days post-sowing; (d) callus after 30 days.

Evaluation of analysis method

Figure 3 shows the cyclic voltammetry responses recorded over 10 consecutive cycles of the electrochemical cleaning process. As described in the experimental section, the working electrode was rinsed before each measurement to prevent analyte interference that could lead to adsorption on the electrode surface; such adsorption may introduce impurities and result in non-stable electrochemical responses²³. The voltammograms exhibit characteristic peaks corresponding to a H_2SO_4 solution at a pure poly-crystalline Pt surface²⁴.

According to Strandberg et al.¹⁰ the voltammogram in Fig. 3 can be divided into four regions: (i) the hydrogen adsorption/desorption region ($\text{Pt} + \text{H}^+ + \text{e}^- \rightleftharpoons \text{Pt} - \text{H}_{\text{ads}}$) between 0.00 and -0.2 vs. Ag/AgCl; (ii) the double layer region between 0.1 and 0.4 vs. Ag/AgCl; (iii) the oxidation region during the anodic scan from 0.7 vs. Ag/AgCl up to the upper potential limit; and (iv) the reduction region during the cathodic scan from at an upper potential limit down to 0.6 Ag/AgCl.

To assess the electrocatalytic activity of Pt in the H_2O_2 reaction, cyclic voltammograms were recorded in a 0.1 mol L^{-1} PBS saturated with N_2 (Fig. 4). When the Pt electrode was cycled within a potential window ranging from 0.7 V to -0.5 V vs. Ag/AgCl, a distinct redox peak was observed at 0.25 V , corresponding to the H_2O_2 reduction reaction. The current magnitude increased proportionally with H_2O_2 concentration, confirming the catalytic activity of the Pt electrode toward H_2O_2 reduction, consistent with prior studies²⁵.

The calibration plot was constructed using chronoamperometry at a potential of -0.3 V vs. Ag/AgCl over a 15 minute period. Figure 5 shows the resulting calibration curve, with the insert displaying the chronoamperogram indicating the electrocatalytic response of the Pt electrode across varying H_2O_2 concentrations ($0.3\text{--}1.4 \mu\text{mol L}^{-1}$). The maximum reduction currents corresponding to each H_2O_2 concentration increased as the potential was adjusted to -0.3 V . However, saturation of the sensor was observed after the addition of $1.4 \mu\text{mol L}^{-1} \text{H}_2\text{O}_2$. The limits of detection and quantification were calculated using the formula $3 \times \text{SD}_{\text{blank}}/\text{slope}$ of the calibration

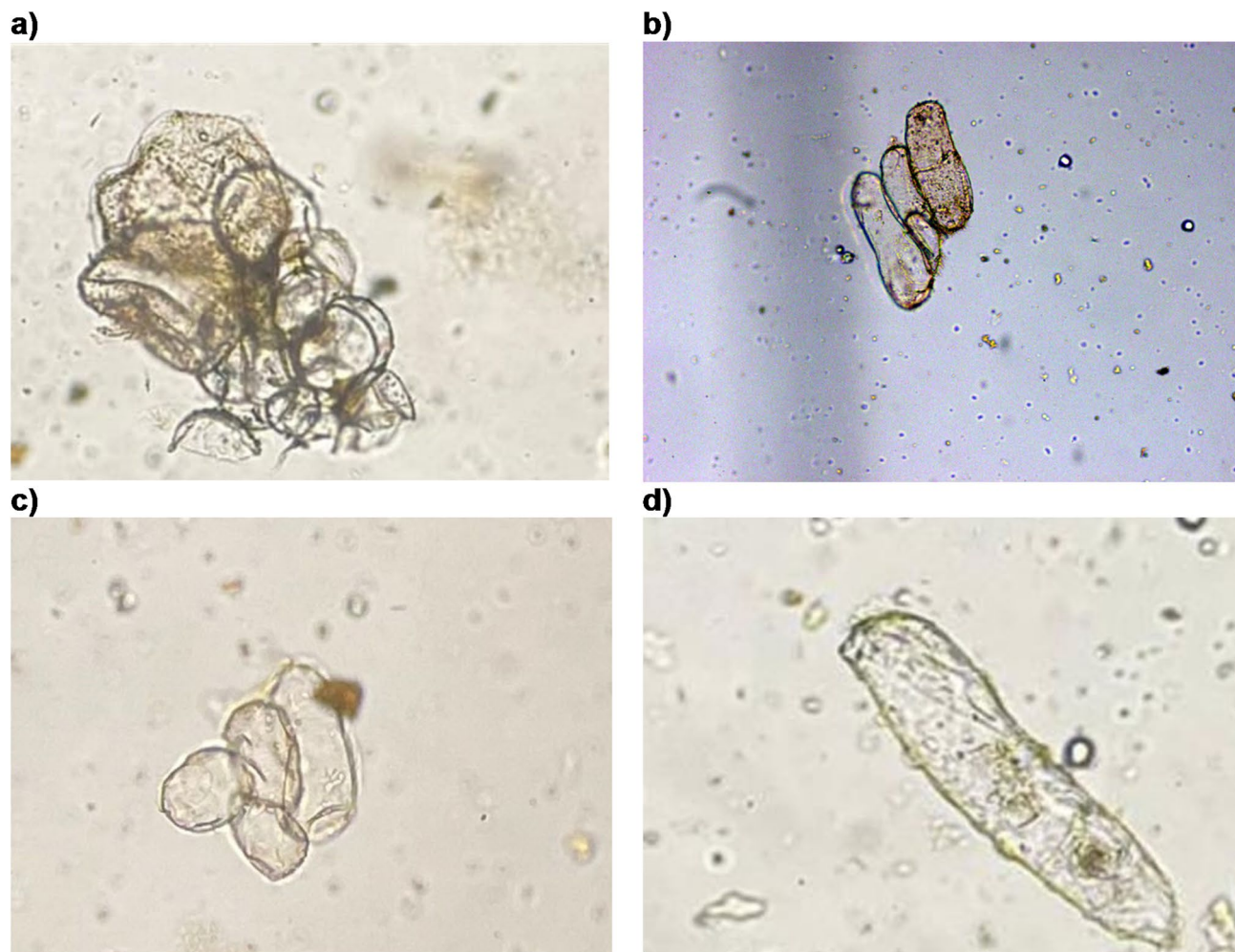


Fig. 2. Microscopic images (10x magnification) of *Theobroma cacao* L. cell suspensions: (a–c) fully dispersed cells and (d) smaller cell clusters.

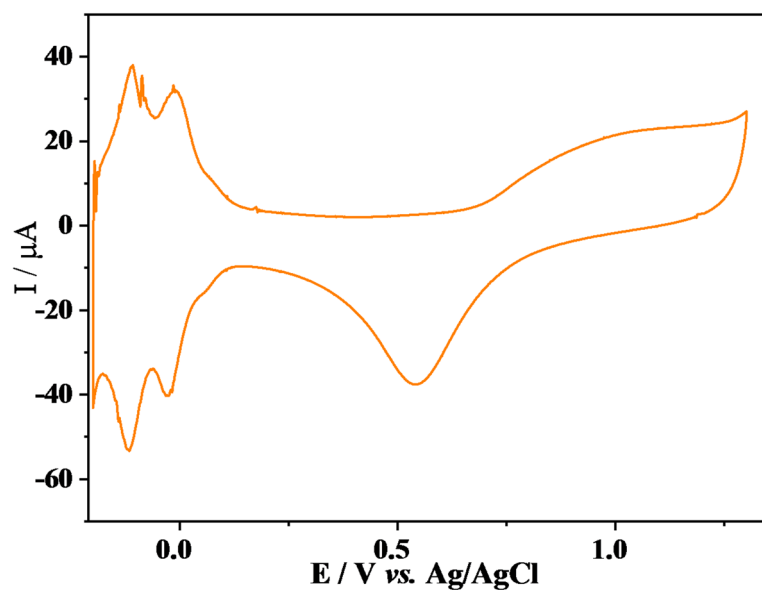


Fig. 3. Cyclic voltammogram of the Pt electrode in $0.5 \text{ mol L}^{-1} \text{ H}_2\text{SO}_4$ at a scan rate of 100 mV s^{-1} , illustrating the electrochemical cleaning process.

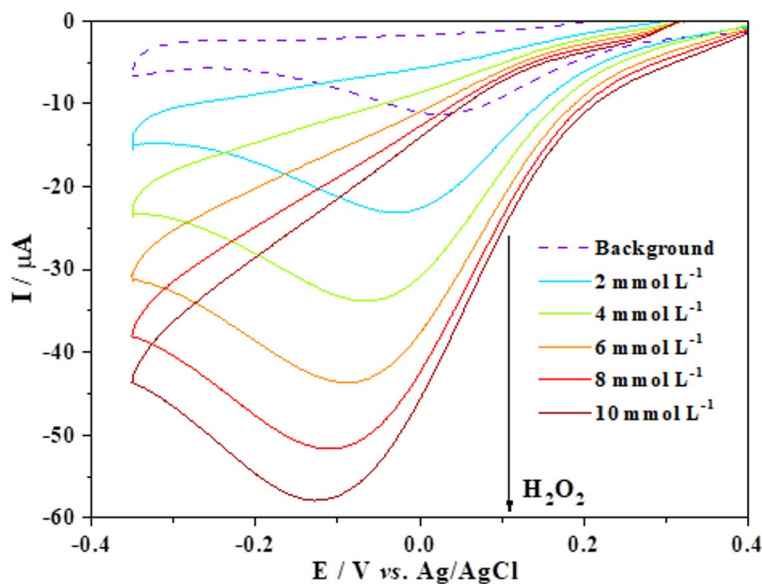


Fig. 4. Cyclic voltammograms of the Pt electrode in phosphate buffer solution (pH 5.7) at a scan rate of 100 mV s^{-1} , recorded with increasing H_2O_2 concentrations.

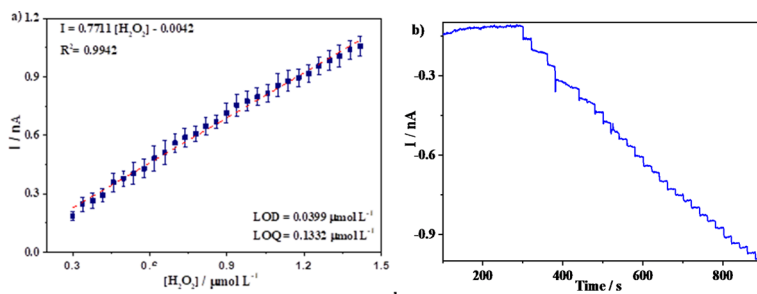


Fig. 5. (a) Calibration plot for H_2O_2 detection on the Pt electrode (3 mm diameter). (b) Chronoamperogram.

Limit of detection ($\mu\text{mol L}^{-1}$)	Limit of quantification ($\mu\text{mol L}^{-1}$)	Coefficient of variation (%)	Recovery (R%)	Parameter
0.012 ± 0.041	0.388 ± 0.001	3.14 ± 0.01	95.73 ± 0.034	Repeatability
0.013 ± 0.043	0.924 ± 0.003	2.94 ± 0.03	99.44 ± 0.024	Reproducibility
0.012 ± 0.050	0.377 ± 0.004	3.17 ± 0.05	105.35 ± 0.014	
0.013 ± 0.020	0.386 ± 0.003	3.45 ± 0.03	98.38 ± 0.017	Mean

Table 2. Limits of detection, quantification, and coefficient of variation based on the repeatability and reproducibility of the method developed to quantify H_2O_2 .

curve and $10 \times \text{SD}_{\text{blank}}$ from the blank/slope of the calibration curve, respectively (Table 2). The analytical sensitivity was determined to be $0.4959 \text{ mA} (\mu\text{mol L}^{-1})^{-1}$.

Hydrogen peroxide quantification in cell suspensions

While ROS are also metabolic by-products in processes such as photosynthesis, respiration, and nitrogen fixation in plants, their concentrations are normally regulated by scavenging agents, including superoxide dismutase, catalase, glutathione reductase, and peroxidase. Thus, living organisms can maintain harmless levels of ROS concentrations during these processes. However, under stress conditions, this balance is disrupted, resulting in the overproduction of ROS and a subsequent oxidative burst a critical and rapid detoxification response in plants^{10,27,28}. Previous studies have indicated that a H_2O_2 concentration of just 2.5 mmol L^{-1} in the medium can initiate a series of chain reactions that irreversibly damage DNA, thereby affecting cells' replication mechanisms²⁹. Conversely, at concentrations exceeding 2.5 mmol L^{-1} , H_2O_2 can damage enzymatic cellular compounds containing Ca^{2+} ³⁰ and attack proteins and lipids within cell membranes, causing lysis³¹. The control

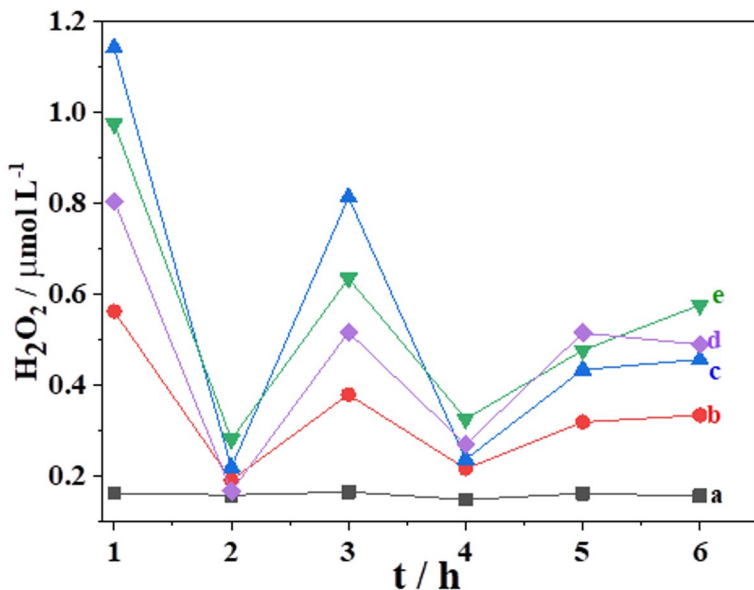


Fig. 6. Relationship between CdSO_4 exposure time and H_2O_2 concentration: (a) $0 \mu\text{mol L}^{-1}$ CdSO_4 ; (b) $5 \mu\text{mol L}^{-1}$ CdSO_4 ; (c) $20 \mu\text{mol L}^{-1}$ CdSO_4 ; (d) $50 \mu\text{mol L}^{-1}$ CdSO_4 ; and (e) $100 \mu\text{mol L}^{-1}$ CdSO_4 .

experiment, in which the suspension was not exposed to CdSO_4 , was conducted in PBS at pH 5.7, resulting in a mean H_2O_2 concentration of $0.16 \mu\text{mol L}^{-1}$ (Fig. 6a). Figure 6b–e illustrates the relationship between generated H_2O_2 concentrations and exposure time in *T. cacao* L. cells subjected to different concentrations of CdSO_4 . There was no change in H_2O_2 concentration in the control medium (Fig. 6a) over 6 h, suggesting that, in the absence of oxidative stress, natural ROS scavenging agents effectively maintain H_2O_2 concentration at a constant level.

After 1 h of the cell suspension's exposure to CdSO_4 solutions, the quantified H_2O_2 at the electrode was considerably higher than that in the unstressed suspension (Fig. 6b–e). Thus, 1 h was determined to be the minimum time required to detect H_2O_2 in the system due to the oxidative stress process. As shown in Fig. 6, the cell suspension's response to increasing CdSO_4 concentrations is consistent with previously reported data³²; specifically, increasing the amount of Cd^{2+} in the medium led to higher H_2O_2 production by cells. The suspension exposed to $5 \mu\text{mol L}^{-1}$ CdSO_4 (Fig. 6b) exhibited the lowest H_2O_2 concentration over time, while the highest concentration corresponded to the suspension exposed to $100 \mu\text{mol L}^{-1}$ CdSO_4 (Fig. 6c). In all cases, peak H_2O_2 production was quantified at 3 h, regardless of CdSO_4 concentration. Overall, Fig. 6 shows that after 1 h of exposure to different CdSO_4 concentrations, H_2O_2 concentrations are higher than those in the control medium, supporting the occurrence of an oxidative burst.

According to the graph shown in Fig. 6, the highest H_2O_2 concentrations after adding CdSO_4 to the cell suspensions occur at 1, 3, and 5 h. Each peak in H_2O_2 concentration can indicate an oxidative burst at the respective CdSO_4 concentration. Conversely, the minimum H_2O_2 concentrations at 2 and 4 h likely correspond to periods wherein the cells gradually recover equilibrium, as these concentrations are the same as or very close to those for the control, $0.16 \mu\text{mol L}^{-1}$ H_2O_2 (Fig. 6a).

The results suggest that the overproduction of H_2O_2 in cell suspensions of *T. cacao* L. seeds was related to the plant's defense mechanism against Cd^{2+} ions. Upon exposure to the metal, cell surface receptors recognize it, stimulating localized H_2O_2 production. H_2O_2 delays germination, allowing cells more time to activate their defense mechanisms, which contributes to resistance to Cd^{2+} stress. However, cell suspension behavior after 5 h of CdSO_4 exposure suggests that *T. cacao* L. seed cells lose their capacity to re-establish equilibrium H_2O_2 concentrations beyond this duration. This is evidenced by the increased production of H_2O_2 in all suspensions, regardless of CdSO_4 concentration, which fails to return to the baseline H_2O_2 concentration observed in the control. Notably, cell suspensions exposed to $100 \mu\text{mol L}^{-1}$ CdSO_4 (Fig. 6c) showed the lowest capacity for recovery.

The addition of H_2O_2 is a commonly used method to induce cellular oxidative stress, typically requiring H_2O_2 concentrations greater than $100 \mu\text{mol L}^{-1}$ ^{33,34}. According to Fig. 6, after 5 h of exposure, cell apoptosis could occur due to the overproduction of H_2O_2 caused by stress from the contaminating metal, thereby impairing the cells' ability to recover. This reaction produces molecular oxygen through the catalase reaction, a very rapid reaction that drastically decreases H_2O_2 concentration within minutes³⁵. Additionally, the results highlight the efficacy of intracellular antioxidant defenses against H_2O_2 .

These findings support the potential of *T. cacao* L. as a bioindicator for Cd contamination in the environment. The observed correlation between Cd exposure and H_2O_2 production suggests that oxidative stress responses in cacao cells can serve as an early warning system for toxic metal pollution. The plant's ability to accumulate Cd and generate a measurable oxidative stress response highlights its suitability for biomonitoring applications, particularly in regions where cacao cultivation is economically and environmentally important. Furthermore,

the progressive loss of cellular recovery capacity under prolonged Cd exposure underscores the potential long-term impacts of toxic metal contamination on cacao plantations.

Integrating electrochemical H₂O₂ quantification into environmental monitoring programs could provide a rapid and sensitive method for detecting metal-induced oxidative stress, reinforcing the role of *T. cacao* L. as a practical and sustainable bioindicator for assessing environmental Cd contamination. Additionally, recent studies have highlighted the critical function of phenolic compounds in plant defense mechanisms against Cd stress. These non-enzymatic antioxidants act as ROS scavengers and metal chelators, thereby mitigating oxidative damage and enhancing stress tolerance⁴². *T. cacao* L. phenolic compounds may play a crucial role in maintaining redox balance under Cd stress, complementing enzymatic defenses. Future studies exploring this interaction could further strengthen the potential of *T. cacao* L. as a biomonitor for Cd contamination.

Conclusion

The determination of H₂O₂ via chronoamperometry using Pt as the working electrode proved to be an effective methodology for Cd quantification, achieving detection and quantification limits of 0.012 and 0.389 μmol L⁻¹, respectively. The findings showed that *T. cacao* L. responds to Cd stress through increased H₂O₂ production, demonstrating its potential as a sedentary bioindicator for environmental contamination. The observed correlation between Cd levels and oxidative stress marker suggests that *T. cacao* L. could serve as an efficient tool for monitoring toxic metal pollution in agricultural regions. Additionally, the results highlight the effectiveness of the plant's defense mechanisms, as evidenced by its immediate oxidative response to Cd-induced stress.

To establish *T. cacao* L. as a bioindicator, field-based studies should be conducted to validate laboratory findings under real environmental conditions. Standardized protocols for H₂O₂ quantification in cacao tissues should be developed to ensure reliable and reproducible results. Moreover, policymakers should consider incorporating *T. cacao* L. into environmental monitoring programs, particularly in regions where cacao cultivation is a major economic activity. Regulatory agencies could leverage these findings to establish early warning systems for Cd contamination, helping to safeguard both agricultural sustainability and public health.

Data availability

Data "available on request": lmfernandez@puce.edu.ec.

Received: 29 January 2025; Accepted: 11 July 2025

Published online: 23 July 2025

References

1. Zhou, Q. et al. An appealing tool for assessment of metal pollution in the aquatic ecosystem. *Anal. Chim. Acta* **606**, 135–150 (2008).
2. El-SiKaily, A. & Shabaka, S. Biomarkers in aquatic systems: advancements, applications and future directions. *Egypt. J. Aquat. Res.* **50**, 169–182 (2024).
3. Biomonitoring of Pollutants in the Global South. Biomonitoring of Pollutants in the Global South. (2024). <https://doi.org/10.1007/978-981-97-1658-6/COVER>
4. Vargas Jentzsch, P. et al. Distinction of Ecuadorian varieties of fermented cocoa beans using Raman spectroscopy. *Food Chem.* **211**, 274–280 (2016).
5. Wexler-Goering, L. & Alvarado-Marenco, P. Fine and flavor cocoa: key aroma compounds and their behavior during processing. *Agronomía Mesoamericana*, **35**, 59679–59679 (2024).
6. Reygaert, W. C. & Reygaert, W. C. An overview of the antimicrobial resistance mechanisms of bacteria. *AIMS Microbiology* **2018** 3:482 4, 482–501 (2018).
7. Mansoor, S. et al. Biochar mediated remediation of emerging inorganic pollutants and their toxicological effects on plant and soil health. *J. Soil. Sci. Plant. Nutr.* **25**, 1612–1642 (2025).
8. Davidova, S., Milushev, V. & Satchanska, G. The Mechanisms of Cadmium Toxicity in Living Organisms. *Toxics* **12**, (2024).
9. Wang, H. et al. Cadmium-induced genomic instability in arabidopsis: molecular toxicological biomarkers for early diagnosis of cadmium stress. *Chemosphere* **150**, 258–265 (2016).
10. Xu, Q. et al. In vivo monitor oxidative burst induced by Cd2+ stress for the oilseed rape (*Brassica Napus* L.) based on electrochemical microbiosensor. *Phytochem Anal.* **21**, 192–196 (2010).
11. Wampash Najamtaí, G. B., Nieves, N., Barriga Castillo, F. M. & Implementación G. R. adecuación y Valoración de Un sistema de climatizado, Para El área de incubación Del laboratorio de micropropagación Del campus Juan Lunardi Cantón paute. *Provincia Del. Azuay* **1** (2011).
12. Baker, C. J. & Mock, N. M. A method to detect oxidative stress by monitoring changes in the extracellular antioxidant capacity in plant suspension cells. *Physiol. Mol. Plant. Pathol.* **64**, 255–261 (2004).
13. Akter, S., Khan, M. S., Smith, E. N. & Flashman, E. Measuring ROS and redox markers in plant cells. *RSC Chem. Biol.* **2**, 1384–1401 (2021).
14. Balladares, C. et al. Physicochemical characterization of *Theobroma cacao* L. sweatings in Ecuadorian Coast. *Emir J. Food Agric.* **28**, 741–745 (2016).
15. Montero-Jiménez, M. et al. Evaluation of the cadmium accumulation in Tamarillo cells (*Solanum betaceum*) by indirect electrochemical detection of Cysteine-Rich peptides. *Molecules* **2019**, **24**, 2196 (2019).
16. Alvarez-Paguy, J., Fernández, L., Bolaños-Méndez, D., González, G. & Espinoza-Montero, P. J. Evaluation of an electrochemical biosensor based on carbon nanotubes, hydroxyapatite and horseradish peroxidase for the detection of hydrogen peroxide. *Sens Biosensing Res* **37**, (2022).
17. Fernández, L. et al. Electrochemical sensor for hydrogen peroxide based on Prussian blue electrochemically deposited at the TiO₂-ZrO₂-Doped carbon nanotube glassy carbon-Modified electrode. *Front. Chem.* **10**, 884050 (2022).
18. Lopes da Silva, A. L. et al. Chemical sterilization of culture medium: A low cost alternative to in vitro establishment of plants. *Scientia Forestalis/Forest Sci.* **41**, 257–264 (2013).
19. Dar, S. A., Nawchoo, I. A., Tyub, S. & Kamili, A. N. Effect of plant growth regulators on in vitro induction and maintenance of callus from leaf and root explants of *Atropa acuminata* royle ex Lindl. *Biotechnol. Rep.* **32**, e00688 (2021).
20. Hesami, M., Daneshvar, M. H., Yoosefzadeh-Najafabadi, M. & Alizadeh, M. Effect of plant growth regulators on indirect shoot organogenesis of *Ficus religiosa* through seedling derived petiole segments. *J. Genetic Eng. Biotechnol.* **16**, 175–180 (2018).

21. Puad, N. I. M., Mze, S. A. I., Azmi, A. S. & Abduh, M. Y. The influence of plant growth regulators and light supply on bitter cassava callus initiation for starch production. *IIUM Eng. J.* **25**, 1–11 (2024).
22. Curtis, W. R. & Emery, A. H. *Plant Cell Suspension Culture Rheology*.
23. Elgrishi, N. et al. A practical beginner's guide to Cyclic voltammetry. *J. Chem. Educ.* **95**, 197–206 (2018).
24. Strandberg, L. et al. Comparison of Oxygen Adsorption and Platinum Dissolution in Acid and Alkaline Solutions Using Electrochemical Quartz Crystal Microbalance. *ChemElectroChem* **9**, (2022).
25. Okada, H., Mizuuchi, R., Sakurada, Y., Nakanishi, S. & Mukouyama, Y. Electrochemical oscillations (Named oscillations H and K) during H₂O₂ reduction on Pt electrodes induced by a local pH increase at the electrode surface. *J. Electrochem. Soc.* **168**, 76512 (2021).
26. Bagur, G., Sánchez-Viñas, M., Gázquez, D., Ortega, M. & Romero, R. Estimation of the uncertainty associated with the standard addition methodology when a matrix effect is detected. *Talanta* **66**, 1168–1174 (2005).
27. Apostol, I., Heinstein, P. F. & Low, P. S. Rapid stimulation of an oxidative burst during elicitation of cultured plant cells: role in defense and signal transduction. *Plant. Physiol.* **90**, 109–116 (1989).
28. Luna, C. M., González, C. A. & Trippi, V. S. Oxidative damage caused by an excess of copper in oat leaves. *Plant. Cell. Physiol.* **35**, 11–15 (1994).
29. Szmidgiero, L. & Studzian, K. H₂O₂ as a DNA fragmenting agent in the alkaline elution interstrand crosslinking and DNA-Protein crosslinking assays. *Anal. Biochem.* **168**(1), 88–93 (1988).
30. Sato, H. et al. Hydrogen peroxide mobilizes Ca²⁺ through two distinct mechanisms in rat hepatocytes. *Acta Pharmacol. Sin.* **30**, 78–89 (2009).
31. Horn, A. & Jaiswal, J. K. Structural and signaling role of lipids in plasma membrane repair. in *Current Topics in Membranes* vol. 84 67–98 Academic Press Inc., (2019).
32. Guo, B., Liu, C., Liang, Y., Li, N. & Fu, Q. Salicylic acid signals plant defence against cadmium toxicity. *International Journal of Molecular Sciences* vol. 20 Preprint at (2019). <https://doi.org/10.3390/ijms20122960>
33. Ransy, C., Vaz, C., Lombès, A. & Bouillaud, F. Use of H₂O₂ to cause oxidative stress, the catalase issue. *Int. J. Mol. Sci.* **21**, 9149 (2020).
34. Park, C. S., Yoon, H. & Kwon, O. S. Graphene-based nanoelectronic biosensors. *J. Ind. Eng. Chem.* **38**, 13–22 (2016).
35. Sule, R. O., Condon, L. & Gomes, A. V. A Common Feature of Pesticides: Oxidative Stress—The Role of Oxidative Stress in Pesticide-Induced Toxicity. *Oxid Med Cell Longev* 5563759 (2022). (2022).

Acknowledgements

The authors thank *ESPE-Ecuador* (Departamento de Ciencias de la Vida y Agricultura) for its technical assistance.

Author contributions

The Author Contributions section is mandatory for all articles, including articles by sole authors. If Conceptualization: L.F.; Data curation: M.J.G.-L., P.B., L.F. and P.E.-M.; Formal analysis: L.F., M.J., and P.E.-M.; Funding acquisition: L.F. and P.E.-M.; Investigation: M.J.G.-L., P.B., L.F., and P.E.-M.; Methodology: M.J.G.-L., M.J., A.O.G and L.F.; Project administration: L.F.; Resources: L.F. and P.E.-M.; Supervision: L.F.; Validation: P.B., L.F., J.D.S. and D.B.-M.; Visualization: A.R., L.F. and P.E.-M.; Roles/Writing - original draft: L.F.; and P.E.-M.; Writing - review & editing: A.R., P.E.-M.

Funding

Dirección de Investigación de la Pontificia Universidad Católica del Ecuador.

Declarations

Competing interests

The authors declare no competing interests.

Additional information

Correspondence and requests for materials should be addressed to L.F. or P.J.E.-M.

Reprints and permissions information is available at www.nature.com/reprints.

Publisher's note Springer Nature remains neutral with regard to jurisdictional claims in published maps and institutional affiliations.

Open Access This article is licensed under a Creative Commons Attribution 4.0 International License, which permits use, sharing, adaptation, distribution and reproduction in any medium or format, as long as you give appropriate credit to the original author(s) and the source, provide a link to the Creative Commons licence, and indicate if changes were made. The images or other third party material in this article are included in the article's Creative Commons licence, unless indicated otherwise in a credit line to the material. If material is not included in the article's Creative Commons licence and your intended use is not permitted by statutory regulation or exceeds the permitted use, you will need to obtain permission directly from the copyright holder. To view a copy of this licence, visit <http://creativecommons.org/licenses/by/4.0/>.

© The Author(s) 2025